# Charge transfer in slow collisions of $O^{8+}$ and $Ar^{8+}$ ions with H(1*s*) below 2 keV/amu

Teck-Ghee Lee,[1,2] M. Hesse,[2,3] Anh-Thu Le,[2] and C. D. Lin[2]
[1]*Physics Division, Oak Ridge National Laboratory, Oak Ridge, Tennessee 37831, USA*
[2]*Department of Physics, Kansas State University, Manhattan, Kansas 66506, USA*
[3]*Physique Quantique CP165/82, Université Libre de Bruxelles, B-1050 Brussels, Belgium*
(Received 21 January 2004; published 6 July 2004)

We calculated the charge-transfer cross sections for $O^{8+}+H$ collisions for energies from 1 eV/amu to 2 keV/amu, using the recently developed hyperspherical close-coupling method. In particular, the discrepancy for electron capture to the $n=6$ states of $O^{7+}$ from the previous theoretical calculations is further analyzed. Our results indicate that at low energies (below 100 eV/amu) electron capture to the $n=6$ manifold of $O^{7+}$ becomes dominant. The present results are used to resolve the long-standing discrepancies from the different elaborate semiclassical calculations near 100 eV/amu. We have also performed the semiclassical atomic orbital close-coupling calculations with straight-line trajectories. We found the semiclassical calculations agree with the quantal approach at energy above 100 eV/amu, where the collision occurs at large impact parameters. Calculations for $Ar^{8+}+H$ collisions in the same energy range have also been carried out to analyze the effect of the ionic core on the subshell cross sections. By using diabatic molecular basis functions, we show that converged results can be obtained with small numbers of channels.

DOI: 10.1103/PhysRevA.70.012702 PACS number(s): 34.70.+e, 31.15.Ja

## I. INTRODUCTION

Electron-capture processes involving impurity gaseous atoms are pivotal in the study of the atomic processes in a controlled fusion reactor. Electron transfer from an H atom to highly charged ions is considered to be one of the rate-determining processes in plasma heating by neutral hydrogen-beam injection. For this reason, many investigations have been carried out to understand the cross sections for the charge transfer between atomic hydrogen and highly charged ions.

Numerous experimental and theoretical studies of charge-transfer cross sections for slow $O^{8+}+H$ collisions have been performed since the early 1980s. The experimental data of Meyer *et al.* [1], Dijkamp *et al.* [2] and Panov *et al.* [3] reported total electron-capture cross sections for energies above 1 keV/amu. These data, which agree with each other to within about a factor of 2, are in good agreement with the total electron cross sections obtained by close-coupling calculations, using either the two-center atomic-orbital (AO) expansion method (Fritsch and Lin [4]) or the molecular-orbital (MO) expansion method (Shipsey *et al.* [5] and of Kimura and Lane [6]). In particular, the experimental data of Meyer *et al.* are in close agreement with the calculation of Fritsch and Lin (AO). However, this general agreement in the total cross section fails to reveal the significant discrepancies in the reported partial electron-capture cross sections among the theories. While electron capture occurs primarily to the $n=5$ states of $O^{7+}$ for collision energies above 1 keV/amu, the theoretical predictions for partial cross sections below 1 keV/amu differ drastically. In the AO calculation of Fritsch and Lin, it was found that the dominant electron capture proceeds to the $n=5$ states, and partial cross sections to the $n=6$ states decrease rapidly with decreasing collision energies. This is in sharp contrast with the calculations carried out by Shipsey *et al.*, where they performed calculations using molecular orbitals as basis functions modified with electron translational factors. They predicted that the $n=6$ states of $O^{7+}$ are predominantly populated for collision energy below 100 eV/amu. A similar calculation performed by Kimura and Lane, also using molecular orbitals as basis functions and some form of electron translational factors, however, obtained results similar to Fritsch and Lin, i.e., the $n=5$ cross section remains the dominant one. Moreover, a relatively more recent calculation by Richter and Solov'ev [7], who used the so-called hidden crossing theory based on the adiabatic molecular energies in the complex $R$ plane, provides $n=5$ and $n=6$ partial cross sections below 1 keV/amu, in reasonable agreement with Shipsey *et al.*

The discrepancies among these elaborate calculations are indeed rather disconcerting. Looking into more details among the theoretical models, the AO calculation of Fritsch and Lin used 46 atomic orbitals, while Shipsey *et al.* used 33 MOs, and Kimura and Lane used 30 MOs. The calculation of Richter and Solov'ev used all the MOs with united-atom quantum numbers $n$ less than 11, i.e., 220 states, and take into account 146 branch points. Thus all the calculations include all the dominant asymptotic $n=5$ and $n=6$ channels of $O^{7+}$. One may want to attribute the discrepancy among the three calculations based on the MOs to different electron translational factors, but this is not obvious since if this is the case the discrepancy would occur at higher collision energies rather than at lower energies. Besides the basis set, one additional complication which is expected to be more important at lower collision energies is the possible trajectory effect in these semiclassical calculations. In some of these calculations curved trajectories were used, while in others trajectories were straight lines. In the semiclassical approximation, the effective interaction potential between the two heavy particles is not uniquely defined. This too may lead to a discrepancy among the theories. To resolve these discrepancies, a full quantal calculation is desirable.

 

In this paper, we employed the recently developed hyperspherical close-coupling method (HSCC) [8] to examine this collision system. The HSCC method is formulated similarly to the perturbed stationary-state (PSS) approximation, but without the well-known difficulties [9,10] in that approach. No additional assumptions are needed beyond the truncation of the number of adiabatic channels included in the calculations. Electron-capture cross sections were calculated from 1 eV/amu up to 2 keV/amu. We confirm that the HSCC results are in better agreement with those of Shipsey *et al.* and of Richter and Solov'ev near 100 eV/amu. Thus we conclude that the AO results of Fritsch and Lin, and the MO calculations of Kimura and Lane, are likely incorrect. In addition, we have also performed AO calculations using the same basis set [i.e., $O^{7+}$ ($n=4,5,6$) and H(1*s*)] employed by Fritsch and Lin, but using straight-line trajectories instead of curved trajectories, at energies above 100 eV/amu. The present AO results are in agreement with Shipsey *et al.* and Richter and Solov'ev. A larger basis set calculation with $n=7$ orbitals has also been employed to ensure for convergence. We found that the contribution of capture into $n=7$ cross sections is merely 1%, thus it appears that the problem with Fritsch and Lin was in the use of curved trajectories. The origin of the discrepancy from Kimura and Lane is not clear.

We have also performed HSCC calculations for $Ar^{8+}+H$ collisions in the same energy region. This is to examine the core effect for low-energy charge-transfer cross sections. In Sec. II we briefly outline the hyperspherical close-coupling theory and the results are presented and discussed in Sec. III. A final conclusion is given in Sec. IV.

## II. THE DIABATIC HYPERSPHERICAL CLOSE-COUPLING METHOD

We employ in this study the hyperspherical close-coupling method recently developed by Liu *et al.* [8]. This method has been proven successful in previous applications [8,11–14] to ion-atom collisions involving systems with one electron and two heavy nuclei (or positive ions with closed-shell electrons). This method has been described in detail in Ref. [8]. Thus we present here only a brief overview and the recent modification to the diabatic basis functions of the HSCC method only.

The collision complex, $O^{8+}+H$, is considered a three-particle system consisting of an electron, a proton, and $O^{8+}$. For $Ar^{8+}+H$, the $Ar^{8+}$ is considered a frozen core. The system is described by mass-weighted hyperspherical coordinates. In the "molecular" frame, the first Jacobi vector $\rho_1$ is chosen to be the vector from $O^{8+}$ to $H^+$, with a reduced mass $\mu_1$. The second Jacobi vector $\rho_2$ goes from the center of mass of $O^{8+}$ and $H^+$ to the electron, with a reduced mass $\mu_2$. The hyperradius $R$ and the hyperangle $\phi$ are defined as

$$R=\sqrt{\frac{\mu_1}{\mu}\rho_1^2+\frac{\mu_2}{\mu}\rho_2^2}, \tag{1}$$

$$\tan\,\phi=\sqrt{\frac{\mu_2}{\mu_1}}\frac{\rho_2}{\rho_1}, \tag{2}$$

where $\mu$ is arbitrary. Another angle, $\theta$, is defined as the angle between the two Jacobi vectors. When $\mu$ is chosen equal to $\mu_1$, the hyperradius $R$ is very close to the internuclear distance between $O^{8+}$ and $H^+$. For $Ar^{8+}$ we treat it as an inert ionic core described by a model potential taken from the early work of Abdallah *et al.* [15]. The model potential has the form

$$V_{Ar^{7+}}(r)=-\frac{1}{r}[8+(10+5.5r)e^{-5.5r}]. \tag{3}$$

We first introduce the rescaled wave function

$$\Psi(R,\Omega,\hat{\omega})=\psi(R,\Omega,\hat{\omega})R^{3/2}\sin\,\phi\cos\,\phi, \tag{4}$$

then the Schrödinger equation takes the form

$$\left(-\frac{1}{2}\frac{\partial}{\partial R}R^2\frac{\partial}{\partial R}+\frac{15}{8}+H_{ad}(R;\Omega,\hat{\omega})-\mu R^2E\right)\Psi=0, \tag{5}$$

where $\Omega\equiv\{\phi,\theta\}$, and $\hat{\omega}$ denotes the three Euler angles of the body-fixed frame with respect to the space-fixed frame. $H_{ad}$ is the adiabatic Hamiltonian. The detailed form of the equations can be found in Liu *et al.* [8].

To solve Eq. (5), we expand the rescaled wave function in terms of normalized and symmetrized rotation function $\tilde{D}$, and body-frame adiabatic basis functions $\Phi_{\mu I}(R,\Omega)$,

$$\Psi(R,\Omega,\hat{\omega})=\sum_{\nu}\sum_{I}F_{\nu I}(R)\Phi_{\nu I}(R,\Omega)\tilde{D}^J_{IM_J}(\hat{\omega}), \tag{6}$$

where $\nu$ is the channel index, $J$ is the total angular momentum, $I$ is the absolute value of the projection of **J** along the body-fixed $z'$ axis and $M_J$ is the projection along the space-fixed $z$ axis. Within this approach, a set of adiabatic channel functions and potential curves are first obtained, which serve as the basis for the expansion (6). For collisions involving many channels, we chose to diabatize curves with sharp avoided crossings with the aim of removing channels which do not couple strongly to the channels of interest. Such a procedure has been developed recently and applied to protonium formation in $\bar{p}+H(1s)$ collisions [16].

The adiabatic and diabatic representations are related by a unitary transformation $\Phi^D=C\Phi^A$, where $\Phi^A$ and $\Phi^D$ are adiabatic and diabatic channel functions, respectively, and $C$ is the unitary transformation matrix. It is well known [17,18] that if the transformation matrix is chosen as the solution of the linear equation

$$CP+\frac{dC}{dR}=0, \tag{7}$$

where the matrix $P$ is given by $P_{ij}=-\langle\Phi_i^A|d/dR|\Phi_j^A\rangle$, then in the diabatic representation all the nonadiabatic coupling terms will vanish. This full diabatic procedure has two drawbacks. First, the matrix elements $P_{ij}$ have to be calculated accurately over the whole range of $R$, which is difficult to do especially in the avoided crossing region. Second, the resulting diabatic curves often deviate too much from the adiabatic potential curves, such that the simplicity of the adiabatic picture can be lost. In the HSCC method as presented in [8], we adopted the smooth/slow-variable discretization (SVD) technique of Tolstikhin *et al.* [19]. In this approach the nonadiabatic coupling matrix $P$ is not calculated, as these couplings

are implicitly included in the overlap matrix between the channel functions. Within the same spirit, our goal is to perform diabatization using only the overlap matrix elements.

In order to solve this problem and avoid the calculation of nonadiabatic couplings, we choose to approximate the derivative with respect to the hyperradius in Eq. (7) by doing a simple difference. The $P_{ij}$ matrix elements are then given by

$$P_{ij} \approx \frac{[\langle \Phi_i^A(R)|\Phi_j^A(R)\rangle - \langle \Phi_i^A(R)|\Phi_j^A(R+\Delta R)\rangle]}{\Delta R} \tag{8}$$

and become proportional to the difference of two overlaps of adiabatic functions at two neighboring points. Similarly, the derivative of the $C$ matrix with respect to hyperradius is replaced by $dC_{ij}/dR \approx C_{ij}(R+\Delta R) - C_{ij}(R)/\Delta R$. By substituting these approximations into Eq. (7), we obtain a simple equation for the $C$ matrix,

$$C_{ij}(R+\Delta R) \approx \sum_k C_{ik}(R)\langle \Phi_k^A(R)|\Phi_j^A(R+\Delta R)\rangle. \tag{9}$$

The $C$ matrix at $R+\Delta R$ is then given by the product of the $C$ matrix at $R$ with the overlaps of adiabatic functions at points $R$ and $R+\Delta R$. Note that the summation in Eq. (9) runs over all channels. This is required to diabatize all the adiabatic potential curves over the whole space of the adiabatic basis. However, our goal is to diabatize only curves with sharp avoided crossings, where usually a small number of channels are involved. Thus we limit the summation in Eq. (9) to these channels. To do so we use a criterion based on the value of the overlaps appearing in Eq. (9). More specifically, we choose to diabatize between two channels $m$ and $j$ when their overlap at two neighboring points is larger than some parameter $\alpha$,

$$|\langle \Phi_m^A(R_{k+1})\Phi_j^A(R_k)\rangle| > \alpha, \tag{10}$$

in a given region of the hyperradial space. The smaller the parameter $\alpha$, the more diabatic the final potential curves. In the present calculations, $\alpha$ was chosen equal to 0.2 and $\Delta R$ was set to 0.1 a.u. The diabatization procedure starts at large distances, where we choose the initial condition for $C$ to be equal to the identity matrix. This means that at large distances, adiabatic and diabatic representations are identical. We then rewrite Eq. (9) as

$$C_{ij}(R_k) \approx \sum_m C_{im}(R_{k+1})\langle \Phi_m^A(R_{k+1})|\Phi_j^A(R_k)\rangle, \tag{11}$$

where the summation over $m$ is limited by Eq. (10). This equation is used to propagate the $C$ matrix down to $R=0$. Once the diabatic basis is obtained, further implementation of diabatic HSCC is straightforward with the adiabatic channel functions being replaced by the diabatic ones. Equation (5) has to be solved for each partial wave $J$ until a converged cross section is reached. Using the numerical procedure introduced in Liu *et al.* [8], such calculations can be easily carried out for many partial waves.

### III. RESULTS AND DISCUSSION

In this paper we apply the HSCC methods to calculate the charge-transfer cross sections for $O^{8+}+H(1s)$ collisions. Figure 1(a) presents the adiabatic hyperspherical potential curves included in the calculation for $R$ up to 24 a.u. All 33 channels from $I=0,1,2$, and 3, that dissociate into the $n=5$ and 6 $O^{7+}$ manifolds, are included. For clarity, only $I=0$ and $I=1$ components are shown. In Fig. 1(b), the *diabatic* curves for the dominant channels for this collision at low energies are shown, including two $I=0$ channels and one $I=1$ channel each from the $n=5$ and $n=6$ manifolds. Even though these are hyperspherical potential curves they are practically identical to the Born-Oppenheimer potential curves.

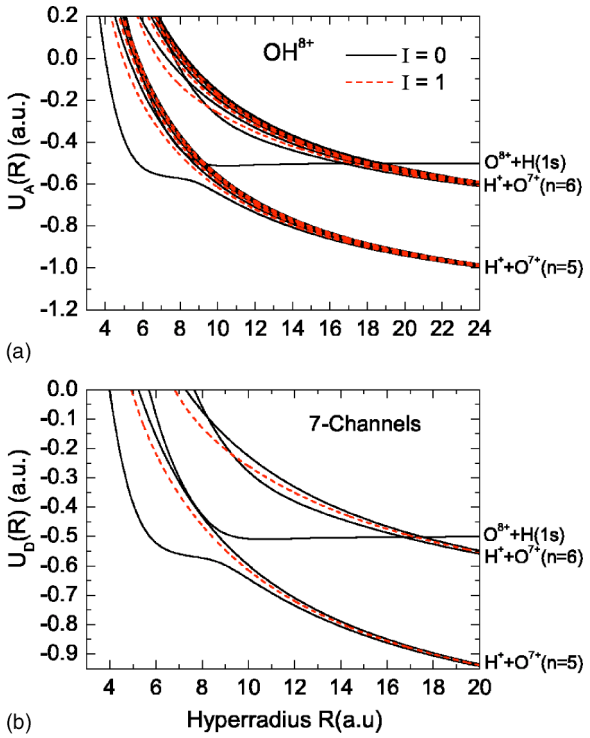


FIG. 1. (a) Hyperspherical adiabatic potential curves for $OH^{8+}$ that dissociate to $O^{7+}$ ($n=5,6$) manifolds. For clarity, only $I=0$ (solid) and $I=1$ (dashed) curves are shown. (b) Dominant seven *diabatic* potential curves.

In Fig. 2(a) we show the partial electron-capture cross sections from 50 eV/amu to 2 keV/amu from the present HSCC calculation. The solid lines are for calculations using the seven channels indicated in Fig. 1(b), while the stars are for calculations carried out using all 33 channels. For the $n=5$ cross sections, the seven-channel calculation is adequate for the whole energy range. For the weaker capture to the $n=6$ channels at energies above 100 eV/amu, the seven-channel results are slightly smaller. We can compare the present values with previous results. They agree well with the 33-state molecular calculation by Shipsey *et al.* The AO calculation of Fritsch and Lin performed in 1984 provides $n=5$ cross sections in agreement with other calculations, but their $n=6$ cross sections are substantially smaller as the collision energy is decreased. In this early calculation, a curved trajectory was introduced to describe the motion of the two heavy particles. To understand the origin of the discrepancy, we carried out the AO calculations using straight-line trajectories. The $n=5$ and $n=6$ cross sections from the new AO calculations, as shown in Fig. 2(a), are in reasonable agree-

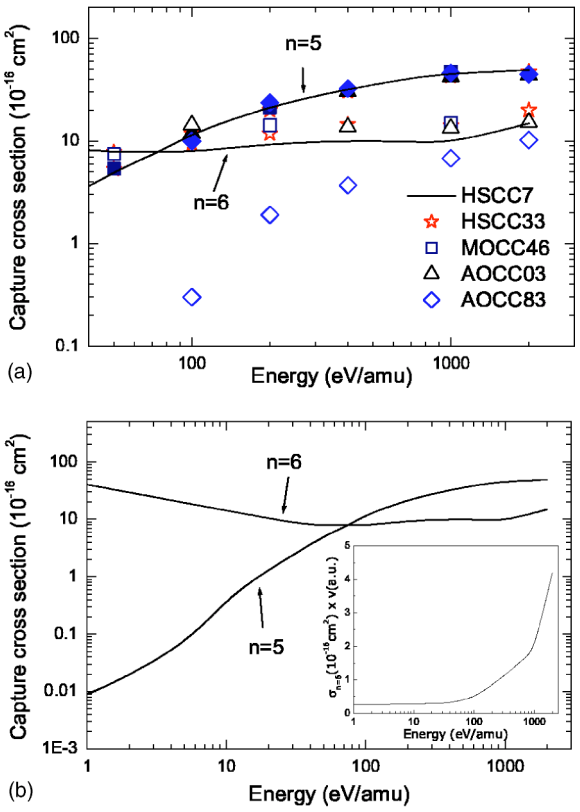


FIG. 2. (a) Partial charge-transfer cross sections for $O^{8+}+H(1s)$ collision as functions of collision energy. Note that the solid symbols are for $n=5$ and the open symbols are for $n=6$. HSCC7, present seven-channel results; HSCC33, present 33-channel results; MO-SGB, MO results by Shipsey *et al.* [5]; AO, present AO results; AO-FL, AO results by Fritsch and Lin [4]. (b) Similar to (a) except for lower range of collision energy. The inset in (b) shows $n=6$ charge-transfer cross section times velocity vs the collision energy.

ment with Shipsey *et al.* This raises the doubt about the curved-trajectory calculations carried out by Fritsch and Lin. Errors could come from an inappropriate effective potential used to describe the curved trajectory for electron capture to the $n=6$ states. On the other hand, the good agreement between straight-line trajectory AO and quantal HSCC results may be attributed to the fact that the collision is dominated at large impact parameters, where the trajectory effect is less significant.

In Fig. 2(b) we present the $n=5$ and $n=6$ cross sections from 1 eV/amu to 2 keV/amu. It shows clearly that the $n=6$ cross sections dominate below 100 eV/amu. The inset which shows the "rate constant," defined to be the relative velocity times cross section, reaches a constant at energies below about 20 eV/amu. Thus the dominant $n=6$ cross sections show the Langevin behavior, i.e., the cross section varies like $1/v$ at low energies, where $v$ is the relative collision velocity.

We now compare the total electron-capture cross section with the experimental data of Meyer *et al.* [1] and the earlier theoretical results, as shown in Fig. 3. Note that the AO calculation of Fritsch and Lin, and the MO-based calculation of Kimura and Lane, are in best agreement with the experiment. However, the results from the present HSCC, and the present AO calculations and the 33-state MO calculations of Shipsey *et al.*, do all suggest that the total capture cross sections are somewhat higher, especially in the low-energy end of Fig. 3.

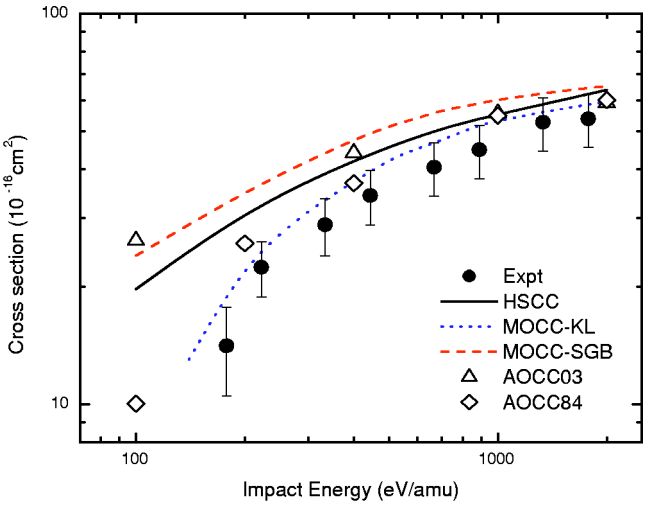


FIG. 3. Total electron-capture cross sections for $O^{8+}+H(1s)$ collision. Theoretical results: (—) denotes the present results of HSCC; (···) the results of Kimura and Lane (Ref. [6]); (−−−) the results of Shipsey *et al.* (Ref. [5]); (◇) the results of AO expansion with curved-line trajectory by Fritsch and Lin (Ref. [4]); (Δ) the present AO expansion with straight-line trajectory. Experimental results are from Meyer *et al.* (Ref. [1]).

In Fig. 4 we analyze the nature of the states populated in the $n=6$ manifold at the collision energies of 10, 100, and 2000 eV/amu. We emphasize that these calculations were carried out with only seven diabatic channels and, as shown in Fig. 2, these seven channels can account for the total $n=5$ and $n=6$ capture cross sections adequately. This is in strong contrast to the earlier MO-based calculations, where a large number of MOs were used in the calculation to "ensure" convergence. On the top frame at 10 eV/amu, we note that the dominant charge-transfer channel is the $I=0$, 6-1 channel (the lowest from the $I=0$ channels in the $n=6$ manifold). It accounts for most of the transition probabilities. Thus, at low energies the collision can be approximated as a two-channel problem. The $I=0$, 6-2 channel contributes less than 1%, while the $I=1$, 6-1 channel contributes less than 5%. Note that electron capture occurs mostly at large impact parameters of about 12–17 a.u., indicating that the avoided crossing near $R=17$ a.u. is the main mechanism for charge transfer at this range of energy. At 100 eV/amu, the $I=1$, 6-1 channel has about the same cross section as from the $I=0$, 6-1 channel, indicating that rotational coupling is very important in this energy region. Note that the $I=0$, 6-2 channel and the $I=1$, 6-1 channel both have relatively larger contributions to the cross section from small impact parameters near 2 a.u. at this energy, but the total cross section still comes mostly from the large impact parameters. At 2 keV/amu, the highest energy used in the present quantal HSCC calculation, the three $n=6$ channels included in the calculation have nearly comparable contributions to the $n=6$ cross section. Clearly, this indicates that electron capture

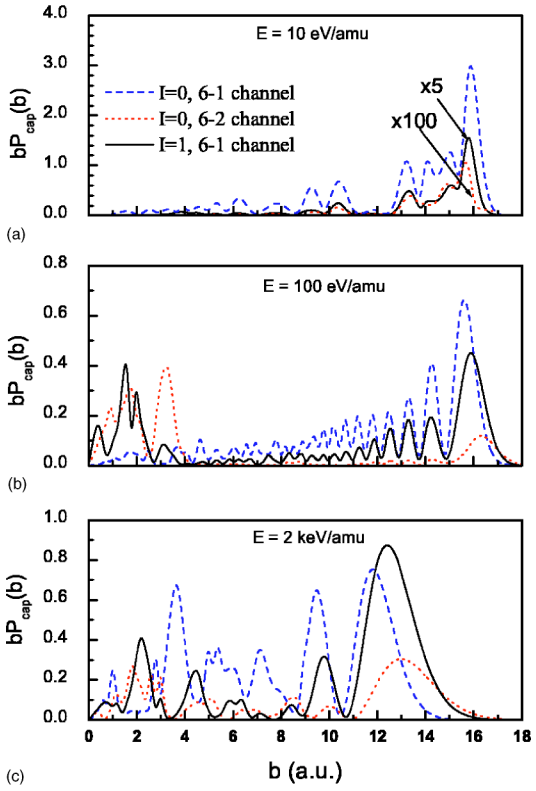


FIG. 4. The evolution of the $bP_{cap}(b)$ vs $b$ with respect to the collision energies. (−−−) and (···) denote the first two $I=0$ channels in the $n=6$ manifold and (—) represents the lowest $I=1$ channel in the $n=6$ manifold for $O^{8+}+H(1s)$ collisions. Note that the 5 and 100 scaling factors only apply to the first panel.

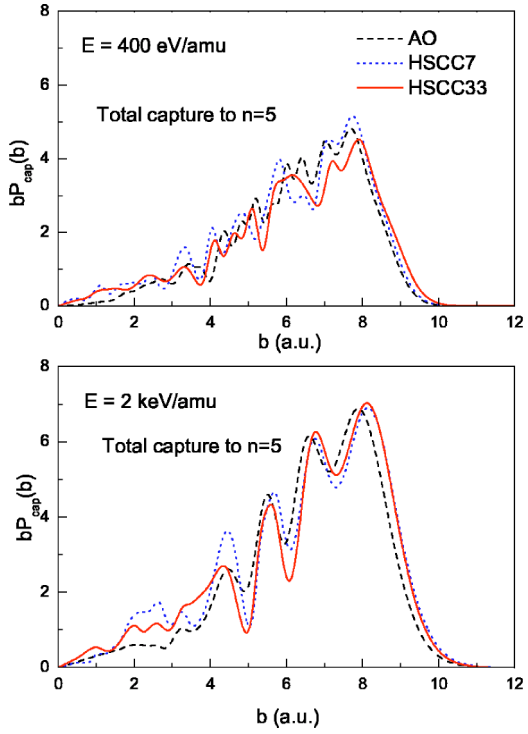


FIG. 5. Comparison of the quantal HSCC and present semiclassical straight-line trajectory AO results for $bP_{cap}$ for the $n=5$ manifold for $O^{8+}+H(1s)$ collisions at a collision energy of $E=400$ eV/amu (top) and 2 keV/amu (bottom).

is not ending up in specific states but rather is fairly well distributed. This means that at this high energy the seven-channel calculation is not quite adequate for the $n=6$ cross sections, as shown in Fig. 2.

In Fig. 5 we compare the $n=5$ electron-capture probabilities from the seven-channel and 33-channel HSCC calculations with the result from the semiclassical AO calculations at $E=400$ eV/amu and 2 keV/amu. In carrying out the AO calculation, straight-line trajectories were used, while the HSCC calculation in principle has included all the possible trajectory effect. Clearly the agreement is quite good and the collision occurs at large impact parameters, suggesting that the effect from a curved trajectory is small. The impact parameter dependence also shows basically a seven-channel calculation is adequate over a large energy range for the dominant channels, and in the higher-energy region either the atomic orbitals or the molecular orbitals can be used as basis functions to describe the electronic motion. Note that we have employed diabatic molecular curves in the HSCC calculations, thus the unimportant channels can be removed easily from the calculation.

We next investigate the collision between $Ar^{8+}$ and $H(1s)$. This system has been investigated at higher collision energies [20], but here we consider collision energies below 2 keV/amu only to examine to what extent the collision dynamics is modified by the fact that the excited $n=6$ and $n=5$ states of $Ar^{7+}$ are no longer degenerate. In Fig. 6(a) the $I=0$ and $I=1$ adiabatic hyperspherical potential curves are shown. The inset zooms into the avoided crossing region of the entrance channel with the $n=6$ states.

We diabatize the sharp avoiding crossings of the entrance channel with the $n=6$ states and the resulting $I=0$ diabatic curves are shown in Fig. 6(b). Note that the entrance channel and the $n=5$ channels do not cross. Comparing Figs. 1 and 5, we notice that for the potential curves in $O^{8+}+H$, the $n=5$ and $n=6$ groups are well separated, and for $Ar^{8+}+H$ the $n=5$ and $n=6$ curves are more evenly distributed. The crossings of the entrance channel with the $n=6$ states occur over a broad range of $R$.

In Fig. 7 we show the calculated $n=5$ and $n=6$ electron-capture cross sections, using 21 molecular states: 11 states of $n=5$ and 6 with $I=0$, and 10 states of $n=5$ and 6 with $I=1$. At higher energies we have used 33 molecular states to confirm that a smaller 21 states are adequate to get converged result. Comparing Fig. 7 with Fig. 2, we note that the relative importance of $n=5$ and $n=6$ cross sections follow a similar pattern. At low energies the capture is predominantly to the $n=6$ states. The inset in Fig. 7 shows that rate constant for the $n=6$ states does not show the Langevin limit until at less than about 1 eV/amu. Furthermore, the $n=5$ cross section, instead of dropping monotonously with decreasing energy, actually curves up below 1 eV/amu. These two "anomalies" are due to our arbitrary separation of cross sections into $n=5$ and $n=6$. Clearly the energy levels for the two manifolds are not well separated and the grouping into $n=5$ and $n=6$ has no real significance.

In Fig. 8, we show the subshell cross sections in terms of the relative collision velocities. Note that at higher velocity

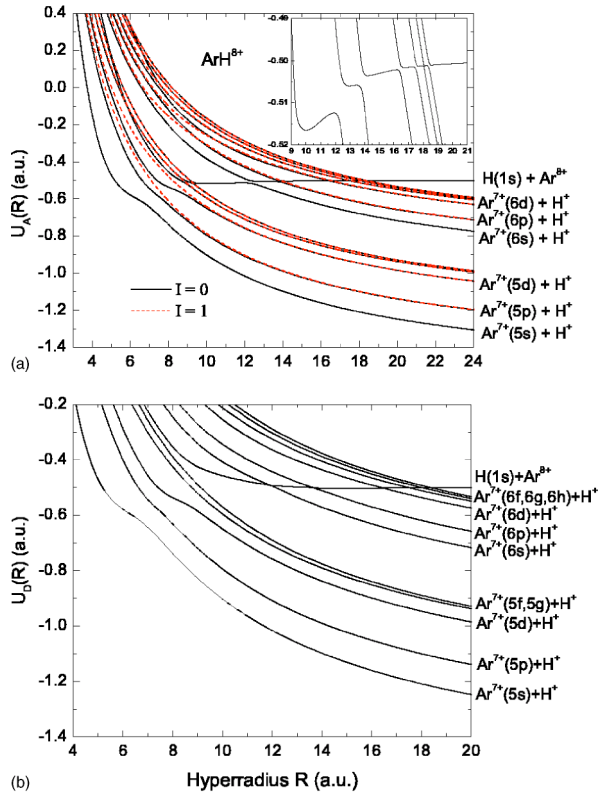


FIG. 6. (a) Hyperspherical adiabatic potential curves for $ArH^{8+}$, which dissociate into $Ar^{7+}(n=5,6)$. Only $I=0$ (solid) and $I=1$ (dashed) channels are shown. The inset gives a zoom in of $n=6$ curves near a series of avoided crossings in the range of $R=10-20$ a.u. (b) Hyperspherical *diabatic* potential curves. For clarity, only $I=0$ curves are shown.

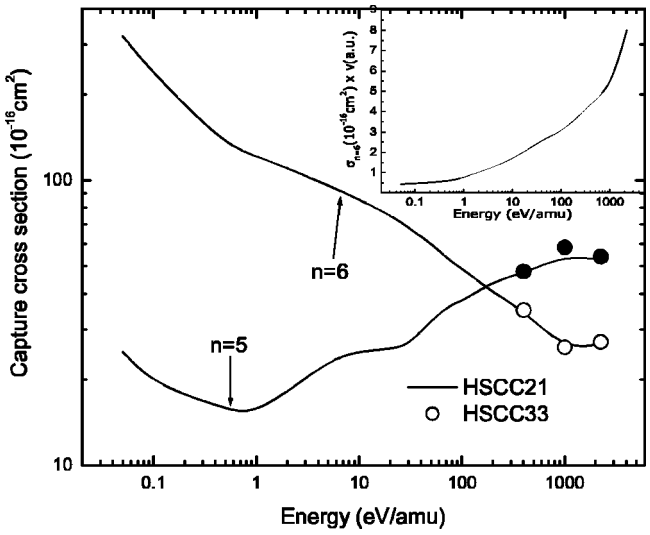


FIG. 7. Partial charge-transfer cross sections for the $Ar^{8+}+H(1s)$ collision system as functions of collision energy. HSCC21, present 21-channel results; HSCC33, present 33-channel results. Note that the solid and open symbols denote the $n=5$ and $n=6$, respectively. The inset shows the $n=6$ charge-transfer cross section times velocity vs the collision energy.

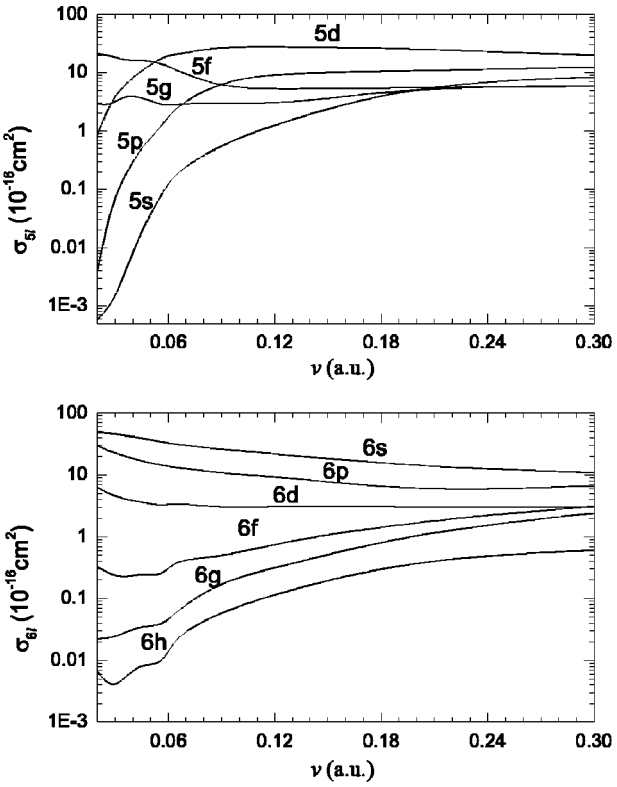


FIG. 8. State selective charge-transfer cross sections for the $Ar^{8+}+H(1s)$ collision system as functions of collision velocity.

the subshell cross sections within a given manifold are relatively comparable. As the collision velocity is decreased, the relative importance of the different subshells changes. The result shows that the diabatic crossing for 6*s* near 12 a.u. (see Fig. 6) and the avoided crossings with 5*f* and 5*g* are the most efficient in transferring the electron to these states. Because 5*f* and 6*s* states are both well populated at the low velocities, there is no simple Langevin limit probably until at even much lower energies.

## IV. CONCLUSIONS

In this paper, the newly developed hyperspherical close-coupling method (HSCC) has been used to calculate electron-capture cross sections for $O^{8+}+H$ and $Ar^{8+}+H$ collisions in the energy range from 1 eV/amu to 2 keV/amu. For $O^{8+}+H$ we were motivated by the long-standing discrepancy between the different elaborate theoretical cross sections. While all these earlier calculations show good agreement in the total cross section and in the $n=5$ cross section, there have been marked differences in the $n=6$ channels, especially at energies below about 100 eV/amu.

Using the HSCC theory, where the motion of the heavy particles is described quantum mechanically, we carried out the calculations from 1 eV/amu to 2 keV/amu—covering the energy region where the controversy exists. Our results agree with those from the molecular approaches of Shipsey *et al.* and Richter and Solov'ev. We believe that the early result of Fritsch and Lin using the AO basis, and of Kimura

and Lane using the MO basis, were incorrect.

To unravel the origin of the discrepancy, we carried out a new AO calculation and as shown in Fig. 2, the new calculations are in agreement with the present HSCC, with Shipsey *et al.* and with Richter and Solov'ev. In the present AO calculation we use straight-line trajectories, while in Fritsch and Lin, a curved trajectory was used. Thus we suspect that the error in the latter was due to the use of a curved trajectory for capture to the $n=6$ states, which occurs at very large internuclear distances. For the discrepancy from Kimura and Lane, we cannot offer any reasonable explanation. Note that the present HSCC calculation also shows that with the use of diabatic basis functions, the $O^{8+}+H$ collision system is rather simple, and calculations using only seven channels are already adequate for the whole energy range covered. This is in strong contrast to the earlier calculations, where the emphasis was to use a much larger molecular basis. The latter of course is needed at higher energies.

We have also performed $Ar^{8+}+H$ calculations to elucidate the difference between these two systems due to the core structure of the projectile. There are no experimental data in the low-energy region investigated in the present paper, but we are confident that the cross sections presented in this paper are reliable.

## ACKNOWLEDGMENTS

This work was supported in part by the Chemical Sciences, Geosciences, and Biosciences Division, Office of Basic Energy Sciences, Office of Sciences, U.S. Department of Energy.

[1] F. W. Meyer, A. M. Howald, C. C. Havener, and R. A. Phaneuf, Phys. Rev. A **32**, 3310 (1985).
[2] D. Dijkamp, D. Čirič, and F. J. de Heer, Phys. Rev. Lett. **54**, 1004 (1985).
[3] M. N. Panov, A. A. Basalaev, and K. O. Lozhkin, Phys. Scr., T **3**, 124 (1983).
[4] W. Fritsch and C. D. Lin, Phys. Rev. A **29**, 3039 (1984).
[5] E. J. Shipsey, T. A. Green, and J. C. Brown, Phys. Rev. A **27**, 821 (1983).
[6] M. Kimura and N. F. Lane, Phys. Rev. A **35**, 70 (1987).
[7] K. Richter and E. A. Solov'ev, Phys. Rev. A **48**, 432 (1993).
[8] C. N. Liu, A. T. Le, T. Morishita, B. D. Esry, and C. D. Lin, Phys. Rev. A **67**, 051801 (2003).
[9] J. B. Delos, Rev. Mod. Phys. **53**, 287 (1981).
[10] M. Kimura and N. F. Lane, Adv. At., Mol., Opt. Phys. **26**, 79 (1989).
[11] C. N. Liu, A. T. Le, and C. D. Lin, Phys. Rev. A **68**, 062702 (2003).
[12] A. T. Le, C. N. Liu, and C. D. Lin, Phys. Rev. A **68**, 021705 (2003).
[13] A. T. Le, M. Hesse, T. G. Lee, and C. D. Lin, J. Phys. B **36**, 3281 (2003).
[14] T. G. Lee, A. T. Le, and C. D. Lin, J. Phys. B **36**, 4081 (2003).
[15] M. A. Abdallah, W. Wolff, H. E. Wolf, E. Sidky, Y. Kamber, M. Stöckli, C. D. Lin, and C. L. Cocke, Phys. Rev. A **57**, 4373 (1998).
[16] M. Hesse, A. T. Le, and C. D. Lin, Phys. Rev. A **69**, 052712 (2004).
[17] B. H. Bransden and M. R. C. McDowell, *Charge Exchange and Theory of Ion-Atom Collisions* (Clarendon, Oxford, 1992), p. 82.
[18] T. G. Heil, S. E. Butler, and A. Dalgarno, Phys. Rev. A **23**, 1100 (1981).
[19] O. I. Tolstikhin, S. Watanabe, and M. Matsuzawa, J. Phys. B **29**, L389 (1996).
[20] J. P. Hansen and K. Taulbjerg, Phys. Rev. A **40**, 4082 (1989).